Acta Cryst. (1973). A29, 415

The Elastic Constants of Monoclinic Potassium Hydrogen Oxalate

BY H. KÜPPERS

Institut für Kristallographie der Universität Köln, 5 *Köln* 41, *Germany* (*BRD*)

(*Received* 21 *December* 1972; *accepted* 23 *February* 1973)

The elastic constants of the monoclinic crystal KHC_2O_4 were measured by diffraction of light by ultrasonic waves. An extremely high elastic anisotropy was observed which is attributed to hydrogen bonds. Force constants derived from the maximum elastic stiffness are compared with force constants of hydrogen bonds and of the oxalate residue determined from infrared measurements.

Introduction

Previous measurements of the elastic constants of acid oxalates (Küppers & Siegert, 1970; Küppers, 1972*b*) revealed an extraordinarily high elastic anisotropy which it has been suggested is caused by the hydrogen bonds between the oxalate residues. In the present paper the elastic constants of another acid oxalate, KHC_2O_4, are reported. This compound should – by analogy with the structure of the crystals previously measured – also exhibit extreme anisotropic effects. It is a further purpose of this study to compare force constants as derived from infrared and Raman spectra with force constants which are deduced from elastic measurements.

Methods and results

Large single crystals were grown from aqueous solution by lowering the temperature from 65 to 35 °C (Küppers, 1972*a*). Sound velocities were measured by the Schaefer–Bergmann method as improved by Haussühl (1956), *i. e.* by diffraction of a light beam by standing ultrasonic waves excited in rectangular specimens (average dimension 1 cm).

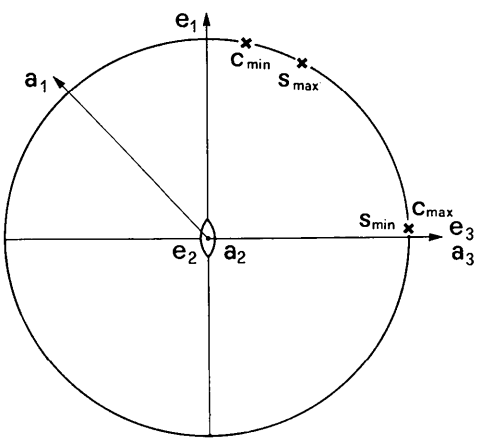

Fig. 1. Stereogram representing the Cartesian axes $\mathbf{e}_i$, the crystallographic axes $\mathbf{a}_i$ and the positions of maximum and minimum longitudinal stiffness c'_{1111} and compliance s'_{1111} (indicated by crosses).

KHC_2O_4 belongs to the monoclinic system. In order to determine the 13 components of the elastic tensor, at least 13 independent measurements are necessary. Additional measurements increase the accuracy. The crystal structure was explored by Hendricks (1935) and was refined by Pedersen (1968) and by Einspahr, Marsh & Donohue (1972). In the present paper the crystallographic coordinate system was chosen according to Groth (1910) and Hendricks (1935) because this is more closely related to the crystal morphology and physical properties than that used by Pedersen (1968) and Einspahr *et al.* (1972). The elastic constants are to be referred to a Cartesian system $\mathbf{e}_i$, with $\mathbf{e}_3$ parallel to $\mathbf{a}_3$, $\mathbf{e}_2$ parallel to $\mathbf{a}_2$, and $\mathbf{e}_1$ parallel to $\mathbf{e}_2 \wedge \mathbf{e}_3$ (see Fig. 1).

In birefringent crystals complications in measuring the sound velocities may occur if the light beam to be diffracted undergoes double refraction (Küppers, 1971). In order to correct for deviations from the usual diffraction geometry caused by this effect, the size and position of the indicatrix must be known. The refractive indices of KHC_2O_4 reported in the literature differ (Winchell, 1954). Therefore, a new determination was made using the prism method. The principal axes of the indicatrix were found to coincide with the Cartesian axes $\mathbf{e}_i$ within the measuring accuracy. The measured refractive indices n_i, referred to the Cartesian axes, for various wavelengths are listed in Table 1.

Table 1. *Refractive indices for various wavelengths*

λ[*nm*]	n_1	n_2	n_3
632	1·372	1·571	1·549
589	1·373	1·574	1·551
546	1·374	1·578	1·555
436	1·379	1·592	1·565

The large optical anisotropy found in KHC_2O_4 requires careful attention to the deviations mentioned above. In order to avoid tedious adjustments and corrections as described previously (Küppers, 1971) the specimens were prepared with such orientation that at least one face-normal lies on principal sections of the indicatrix. Then at least one ray exists (with polarization perpendicular to the principal section) which does not undergo double refraction. If this ray is chosen for the measurement, no correction is needed. Such choice

of measuring directions is also recommended for future measurements of elastic constants in monoclinic as well as triclinic crystals.

21 sound velocities were measured at 20 °C along 12 different, uniformly distributed directions. The elastic constants (stiffnesses) c_{mn} calculated from these velocities by the method described by Haussühl & Siegert (1969) are listed in Table 2. A density of 2·064 g cm^{-3} was assumed. Table 2 also contains the elastic compliances s_{mn} which were obtained from the c_{mn} by matrix inversion. The errors were obtained from the least-squares computation. The volume compressibility, $K = -\partial \log V/\partial p = \sum_{k,l=1}^{3} s_{iikk}$ is found to be $K = 6{\cdot}85 \cdot 10^{-12}$ cm^2 dyne^{-1}.

The extrema of longitudinal stiffness, $c'_{1111} = a_{1i}a_{1j}a_{1k}a_{1l}c_{ijkl}$, were derived by rotation of the reference system within the mirror plane. The maximum and minimum values and the direction cosines of the corresponding directions (given in brackets) are:

$$c'^{\max}_{1111} = 8{\cdot}797 \cdot 10^{11}\text{dyne cm}^{-2}(0{\cdot}0419;\ 0{\cdot}0;\ 0{\cdot}9991)$$
$$c'^{\min}_{1111} = 1{\cdot}468 \cdot 10^{11}\text{dyne cm}^{-2}(0{\cdot}9753;\ 0{\cdot}0;\ 0{\cdot}2121).$$

Extremal values of the **s** tensor and corresponding direction cosines were found to be:

$$s'^{\min}_{1111} = 1{\cdot}234 \cdot 10^{-12}\text{cm dyne}^{-1}(0{\cdot}0454;\ 0{\cdot}0;\ 0{\cdot}9990)$$
$$s'^{\max}_{1111} = 14{\cdot}41 \cdot 10^{-12}\text{cm dyne}^{-1}(0{\cdot}8805;\ 0{\cdot}0;\ 0{\cdot}4741).$$

While $s'^{\min}_{1111}$ almost exactly coincides with $c'^{\max}_{1111}$, $s'^{\max}_{1111}$ is shifted by a considerable amount toward [001]. The respective directions are indicated in Fig. 1 by crosses.

Discussion

Anisotropy

The elastic anisotropy which may be defined as the ratio of maximum to minimum longitudinal stiffness c'_{1111} (or longitudinal compliance s'_{1111}) has the following magnitude in the present case:

$$\frac{c'^{\max}_{1111}}{c'^{\min}_{1111}} = 6{\cdot}0; \qquad \frac{s'^{\max}_{1111}}{s'^{\min}_{1111}} = 11{\cdot}6.$$

These are the largest elastic anisotropies observed hitherto in crystals. Respective values of $c'^{\max}_{1111}/c'^{\min}_{1111}$ and $s'^{\max}_{1111}/s'^{\min}_{1111}$ (given in brackets) for other crystals exhibiting high elastic anisotropies are: tartaric acid: 5·2 (5·0) (Mason, 1950), ammonium and potassium tetroxalate dihydrate: 4·7 (7·0) and 4·2 (7·2) (Küppers & Siegert, 1970), ammonium hydrogen oxalate hemihydrate: 4·6 (5·8) (Küppers, 1972*b*).

A common characteristic of the crystal structures of the compounds listed above is the formation of hydrogen bonds which preferentially extend in one direction This direction could be correlated with the direction of maximum elastic stiffness (Küppers, 1972*b*).

In the crystal structure of KHC_2O_4 (space group $P2_1/c$) the arrangement of the oxalate residues and the direction of the hydrogen bonds is demonstrated by Fig. 2 which was drawn according to Einspahr, Marsh & Donohue (1972). The structure consists of parallel chains of hydrogen oxalate ions joined by hydrogen bonds and extending in the [001] direction. These chains are linked transversely by K–O electrostatic forces, the K^+ ion being coordinated by seven oxygens. The average plane made up by the six atoms of the C_2O_4 group lies nearly normal to $\mathbf{e}_1$. Because five of seven K–O bonds are employed to link oxalate residues mutually within their average planes, a layer-like structure is achieved, as may be seen in Fig. 2. As a consequence, a pronounced cleavage is observed at (100). Only two K–O bonds, designated *A* and *B* in Fig. 2, contribute to the mutual cohesion of the layers.

These structural characteristics readily allow one to

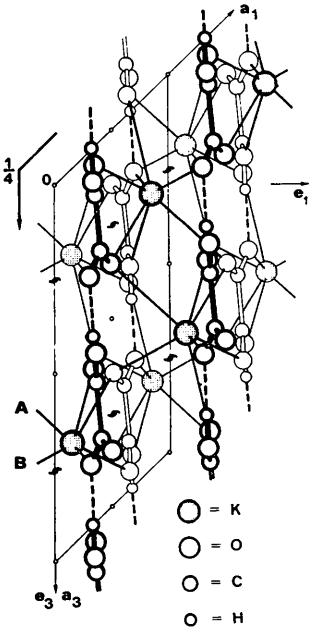

Fig. 2. Perspective view of the structure of KHC_2O_4 as seen down the $\mathbf{a}_2$ axis. Bold circles represent atoms in the upper portion, faint circles those in the lower portion of the unit cell.

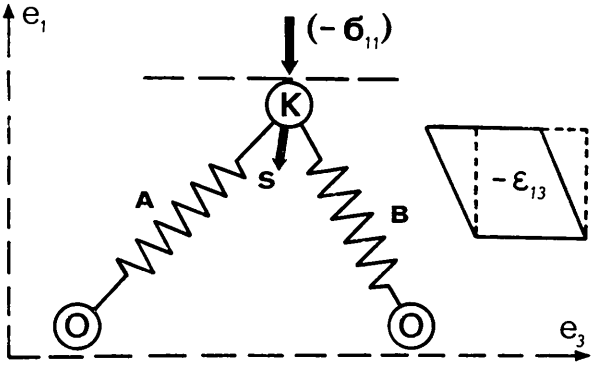

Fig. 3. Schematic representation of the bonds connecting the layers.

explain the main features of elastic behaviour. The graduation of the principal constants, c_{11}, c_{22}, c_{33}, follows from the fact that the structure is primarily composed of firm layers which themselves consist of even stronger chains. Hence, maximum elastic stiffness is determined by the direction of the hydrogen-bonded chains parallel to [001]. Minimum elastic stiffness should be found approximately perpendicular to the layers, *i. e.* parallel to $\mathbf{e}_1$. The shift of the measured minimum (Fig. 1) toward $\mathbf{e}_3$ might be explained by the different inclinations of bonds *A* and *B* relative to $\mathbf{e}_1$ (*cf.* Figs. 2 and 3). Since the force constant is a second-rank tensor, the magnitude of each bond strength decreases with $\cos^2\varphi$ on rotation of the reference system by φ. Assuming central forces and equal force constants for *A* and *B*, a minimum in the resultant force constant occurs between the directions of *A* and *B* in a direction which has shifted towards bond *A*.

The large strength of the chains also explains the relative magnitudes of the constants s_{12}, s_{13} and s_{23}. If a stress σ_{11} or σ_{22} is applied to the crystal, the chains allow only a small strain ε_{33}. Therefore, the constants s_{13} and s_{23} (*i. e.* those containing index 3) are smaller than s_{12} which relates the strain ε_{22} to the stress σ_{11} and ε_{11} to σ_{22}.

Since bonds *A* and *B* are the weakest parts of the structure, further consequences can be deduced from their asymmetric configuration relative to $\mathbf{e}_1$. In Fig. 3, an upper layer is represented by an atom K, a lower by two oxygens O. The layers are assumed to be rigid. If a pressure, $-\sigma_{11}$, due to the force represented by the arrow in Fig. 3, is applied, the upper plane will shift to the left, as indicated by a second arrow S. Thus, a negative shear strain results (a rectangular area will become deformed into a rhombus as drawn in the right part of Fig. 3). Therefore, the compliance $s_{15}=s_{1113}$, which is defined by $\varepsilon_{13}=s_{1311}\sigma_{11}$, should be positive, which is in agreement with the value determined experimentally (*cf.* Table 2). The layerlike structure also accounts for the relative magnitudes of the three shear coefficients, c_{44}, c_{55}, and c_{66}. Shear strains ε_{12} and ε_{13} result when the layers are displaced one relative to the other, parallel to $\mathbf{e}_3$ or $\mathbf{e}_2$. The appropiate resistances occuring during such deformation, c_{55} and c_{66}, are evidently lower than c_{44} which corresponds to a torsion within the layers.

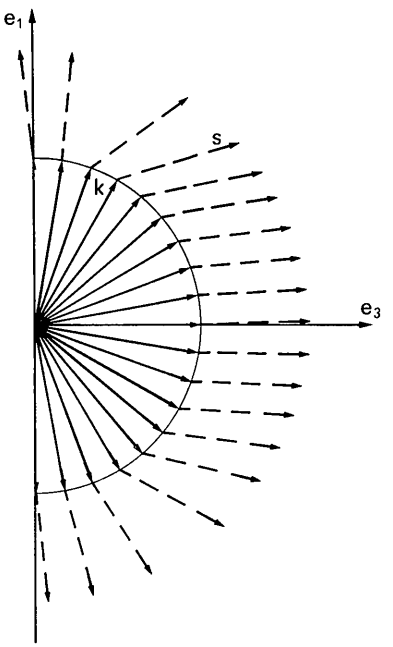

Fig. 4. Propagation directions **k** (bold vectors) with corresponding displacement vectors **s** (dashed) of quasi-longitudinal waves within the mirror plane.

As a consequence of the high elastic anisotropy, extraordinary phenomena concerning the propagation of elastic waves appear. In this case also the predominance of direction $\mathbf{e}_3$ becomes evident. Fig. 4 shows the displacement vectors (dashed) due to different propagation directions (bold vectors) of quasi-longitudinal waves within the mirror plane. Evidently, within a large angular interval the displacement is nearly parallel to $\mathbf{e}_3$. Therefore, between $\mathbf{e}_1$ and $\mathbf{e}_3$, extreme deviations from purely longitudinal character occur. A wave propagating in a direction inclined by 30° to $\mathbf{e}_1$ (towards $\mathbf{e}_3$) possesses a displacement vector which is inclined by 44·5° to the propagation direction.

Fig. 5 shows the (010) section of the slowness surface of quasi-longitudinal waves. The normals to this curve have the directions of the corresponding rays (directions of energy flux). Again, within a large angular interval, the energy flux is nearly parallel to $\mathbf{e}_3$. Extraordinarily strong deviations from collinearity are observed in the interval between $\mathbf{e}_1$ and $\mathbf{e}_3$: when a quasi-longitudinal wave propagates in a direction inclined at 30° to $\mathbf{e}_1$ (as indicated in Fig. 5), the corresponding ray is inclined by about 52° to the wave normal.

Force constants

The qualitative graduation of the three principal constants, c_{11}, c_{22}, and c_{33}, was already made plausible in the previous section. For a quantitative explanation the interatomic potentials must be known. These are, for ionic interaction in complicated structures, not known with a sufficient accuracy. Therefore, we merely note that the values of c_{11} and c_{22} which are predominantly

Table 2. *Elastic stiffnesses* c_{mn}($\times 10^{11}$ dyne cm^{-2}), *relative errors* $\Delta c_{mn}/c_{mn}$ *and elastic compliances* s_{mn}($\times 10^{-12}$ cm^2 dyne^{-1}) *of* KHC_2O_4 *at* 20 °C

mn	11	22	33	12	13	23	44	55	66	15	25	35	46
c_{mn}	1·563	4·446	8·771	1·550	0·824	1·709	1·744	0·360	0·461	−0·150	−0·010	0·309	0·010
$\Delta c/c$	0·4%	0·2%	0·2%	0·8%	1·8%	0·6%	0·4%	1·5%	1·5%	2·7%	–	1·4%	–
s_{mn}	10·556	3·590	1·297	−3·484	−0·479	−0·334	5·735	30·823	21·677	4·704	−1·060	−1·322	−0·126

caused by ionic forces are in the range which is usually observed in salts of organic acids (Bechmann, 1966, 1969; Küppers, 1972*b*). But c_{33}, which is out of the usual range and which is chiefly caused by the stiffness of the chains, can be correlated with other physical properties, *i.e.* with molecular force constants which have been determined from infrared and Raman measurements. Therefore, in the following, the stiffness of the chains as deduced from the elastic constant c_{33} will be compared with the stiffness as calculated from force constants. Molecular force constants have also been used by Jaswon, Gillis & Mark (1968) in order to determine the theoretical stiffness of crystalline native cellulose.

In KHC_2O_4, the longitudinal stiffness of the chain (see Fig. 6) is essentially determined: (*a*) by the stiffness of the hydrogen bond O(4)–H–O(2) which is inclined only by 2° to the chain direction $\mathbf{e}_3$ and which is a composite of two stretching constants f_{OH} and f_H, (*b*) by a force constant f_{COO} which is due to the bending of the O(2)–C(1)–C(2) bonds, and (*c*) by a force constant f_{COOH} which is due to the bending of the C(1)–C(2)–O(4) bonds. The resultant force constant $\bar{f}$ of the constituent unit is given by

$$1/\bar{f}=1/f_H+1/f_{OH}+1/f_{COO}+1/f_{COOH}\,. \qquad (1)$$

Force constants of hydrogen bonds of type O···H–O have been determined in different compounds from infrared and Raman spectra by Nakamoto, Sarma & Ogoshi (1965). A strong dependence on O···O distance and on the collinearity of the O(4)–H bond with the lone-pair orbital of the O(2) atom (Ogoshi & Nakamoto, 1966) has been observed. Since, in KHC_2O_4, angle C(1)–O(2)–O(4) is found to be 123°, this collinearity is assured. Interpolating the measurements of Nakamoto *et al.* (1965), a stretching force constant f_H of about $0{\cdot}95\,.\,10^5$ dyne cm^{-1} and f_{OH} of about $2{\cdot}52\,.\,10^5$ dyne cm^{-1} is estimated.

Force constants of the oxalate ion as well as of oxalic acid have been derived from infrared and Raman measurements by Murata & Kawai (1956) who supposed an Urey–Bradley force field. For the case of a load applied parallel to $\mathbf{e}_3$ the following simplifying assumptions are made: (1) the stretching constants K(C–O) and K(C–C), which are considerably larger than all bending constants H and repulsive constants F, shall be neglected; (2) the C–C direction is not changed. Then, from simple considerations the following force constants may be derived for the COO group and the COOH group, using the potential constants given by Murata & Kawai (1956):

$$f_{COO}=1{\cdot}04\,,\quad f_{COOH}=1{\cdot}26\,.\,10^5\ \text{dyne cm}^{-1}.$$

These constants relate the displacement parallel to $\mathbf{e}_3$ with a force which acts also parallel to $\mathbf{e}_3$. According to equation (1), from these force constants the force constant $\bar{f}$ of the whole hydrogen oxalate unit can be deduced:

$$\bar{f}=0{\cdot}31\,.\,10^5\ \text{dyne cm}^{-1}.$$

On the other hand, f will now be estimated from the macroscopic elastic stiffness parallel to $\mathbf{e}_3$. If a rectangular specimen is subjected to a stress σ_{33}, the resulting strain ε_{33} is determined by

$$\varepsilon_{33}=s'_{3333}\sigma_{33}\,. \qquad (2)$$

For a single spring, the displacement Δl resulting from the application of a force K (both in the direction of the spring axis) is given by $\Delta l=K/f$. Dividing K by the area F required by one spring (*i.e.* 'cross section' of one oxalate residue) yields the stress $\sigma=K/F$. Strain ε is given by the ratio $\Delta l/l$, l being the length of the spring (*i.e.* the distance between two adjacent oxalate residues in the chain). Thus:

$$\varepsilon\,.\,l=\frac{F\,.\,\sigma}{f}\,.$$

By comparison with equation (2), the following expression for f is obtained:

$$f=\frac{F}{s\,.\,l}\,. \qquad (3)$$

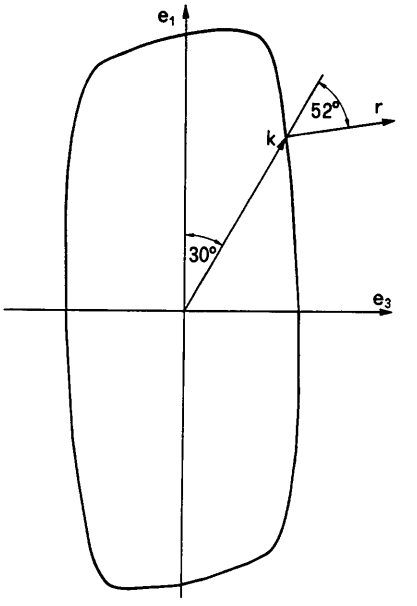

Fig. 5. (010) section of the slowness surface. **r** = energy flux vector due to wave normal **k**.

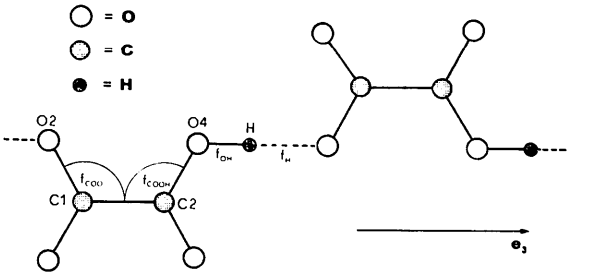

Fig. 6. Arrangement of the hydrogen oxalate ions linked by hydrogen bonds.

In the case of KHC_2O_4, $l=5{\cdot}1$ Å ($=a_3/2$), $F=20$ Å^2, and $s=1{\cdot}3\,.\,10^{-12}$ cm^2 dyne^{-1}. These values yield a force constant $f=0{\cdot}30\,.\,10^5$ dyne cm^{-1}, which is in reasonable agreement with the value $\bar{f}$ derived from force constants as determined from optical measurements.

The actual value of $\bar{f}$ should be somewhat lower because the influence of some force constants, which contribute to an increase of the compliance of the whole unit, was neglected. On the other hand, f, as derived from the elastic constants, is not only caused by the forces given in Fig. 6 but also, to a smaller extent, by some ionic forces due to the cation.

Cauchy relations

According to Haussühl (1967), the deviations from Cauchy relations constitute a second-rank tensor g_{rs} which represents information about bonding characteristics. In the case of KHC_2O_4 the components of the reduced tensor $g^*_{rs}=g_{rs}\,.\,K$ (with K=volume compressibility) have the following values:

$$g^*_{11}=-0{\cdot}024;\ g^*_{22}=0{\cdot}318;\ g^*_{33}=0{\cdot}746;\ g^*_{13}=0{\cdot}014\ .$$

The principal axes of this tensor nearly coincide with the Cartesian system. Here also an appreciable anisotropy is observed. Characteristically, g^*_{11}, which represents the forces in the cleavage plane (100), is found to have the lowest value. A similar behaviour is found in gypsum (Haussühl, 1967).

The author is deeply indebted to Professor Dr S. Haussühl for making experimental arrangements available and for critical remarks. Thanks are also due to Dr H. Siegert whose computer program was used and to Professor Dr H. Pettersen for reading the manuscript.

References

BECHMANN, R. (1966, 1969). *Elastic, Piezoelectric, Piezooptic and Electrooptic Constants of Crystals. Landolt-Börnstein. New Series*, Group III, Vols. 1 and 2. Berlin, Heidelberg, New York: Springer.

EINSPAHR, H., MARSH, R. E. & DONOHUE, J. (1972). *Acta Cryst.* B**28**, 2194–2198.

GROTH, P. (1910). *Chemische Kristallographie*. Vol. III. Leipzig: Engelmann.

HAUSSÜHL, S. (1956). *Naturwissenschaften*, **43**, 394–395.

HAUSSÜHL, S. (1967). *Phys. kondens. Mater.* **6**, 181–192.

HAUSSÜHL, S. & SIEGERT, H. (1969). *Z. Kristallogr.* **129**, 142–146.

HENDRICKS, S. B. (1935). *Z. Kristallogr.* **91**, 48–64.

JASWON, M. A., GILLIS, P. P. & MARK, R. E. (1968). *Proc. Roy. Soc.* A**306**, 389–412.

KÜPPERS, H. (1971). *Acta Cryst.* A**27**, 316–322.

KÜPPERS, H. (1972*a*). *J. Cryst. Growth*, **15**, 89–92.

KÜPPERS, H. (1972*b*). *Acta Cryst.* A**28**, 522–527.

KÜPPERS, H. & SIEGERT, H. (1970). *Acta Cryst.* A**26**, 401–405.

MASON, W. P. (1950). *Piezoelectric Crystals and their Applications to Ultrasonics*. Princeton: Van Nostrand.

MURATA, H. & KAWAI, K. (1956). *J. Chem. Phys.* **25**, 589–590.

NAKAMOTO, K., SARMA, Y. A. & OGOSHI, H. (1965). *J. Chem. Phys.* **43**, 1177–1181.

OGOSHI, H. & NAKAMOTO, K. (1966). *J. Chem. Phys.* **45**, 3113–3120.

PEDERSEN, B. F. (1968). *Acta Chem. Scand.* **22**, 2953–2964.

WINCHELL, A. N. (1954). *The Optical Properties of Organic Compounds*. New York: Academic Press.

Acta Cryst. (1973). A**29**, 419

An Automated Deconvolution of the Patterson Synthesis by Means of a Modified Vector-Verification Method. Its Application to Some Heavy-Atom Patterson Functions

BY A. T. H. LENSTRA* AND J. C. SCHOONE

Laboratory for Crystal Chemistry, Rijksuniversiteit Utrecht, The Netherlands

(*Received* 2 *December* 1971; *accepted* 25 *January* 1973)

A general scheme for the deconvolution of the Patterson-vector map is discussed, in which no structural information is needed. It appears to be possible to overcome the difficulties arising from vector overlap and vector coincidence. The vector-verification method is extended so as make it possible to locate every configuration of a small, fixed number of atoms, for which the complete corresponding vector set is present in the Patterson function. A criterion is defined which expresses the reliability of each configuration, making it possible to recognize the correct one.

1. Introduction

We employed the Patterson superposition method to develop an automated structure-determination procedure, in which no *a priori* structural information is needed (Lenstra, 1969). Having but restricted computer facilities available it was not possible to handle the symmetry minimum function (Simpson, Dobrott & Lipscomb, 1965) adequately. For this reason we have used the vector-verification method (Mighell & Jacobsen, 1963).

* Present address: Universitaire Instelling Antwerpen, departement Scheikunde, Universiteitsplein 1, 2610 Wilrijk, Belgium.